HHS Public Access

Author manuscript

Oncogene. Author manuscript; available in PMC 2013 February 27.

Published in final edited form as:

Oncogene. 2012 April 12; 31(15): 1923–1937. doi:10.1038/onc.2011.379.

Oncogenic YAP promotes radioresistance and genomic instability in medulloblastoma through IGF2-mediated Akt activation

Africa Fernandez-L[1], **Massimo Squatrito**[1], **Paul Northcott**[2], **Aashir Awan**[3], **Eric C. Holland**[1], **Michael D. Taylor**[2], **Zaher Nahlé**[3], and **Anna Marie Kenney**[3,*]

[1]Department of Cancer Biology and Genetics, Memorial Sloan-Kettering Cancer Center, New York, NY 10021

[2]Division of Neurosurgery, Program in Developmental and Stem cell Biology, Arthur and Sonia Labatt Brain Tumor Research Center, Hospital for Sick Children, University of Toronto, Toronto, Ontario, Canada

[3]Departments of Neurosurgery and Cancer Biology, Vanderbilt University, Nashville Tennessee 37232

Abstract

Radiation therapy remains the standard of care for many cancers, including the malignant pediatric brain tumor medulloblastoma. Radiation leads to long-term side effects, while radio-resistance contributes to tumor recurrence. Radio-resistant medulloblastoma cells occupy the peri-vascular niche. They express Yes-associated protein (YAP), a Sonic hedgehog (Shh) target markedly elevated in Shh-driven medulloblastomas. Here we report that YAP accelerates tumor growth and confers radio-resistance, promoting ongoing proliferation after radiation. YAP activity enables cells to enter mitosis with un-repaired DNA through driving IGF2 expression and Akt activation, resulting in ATM/Chk2 inactivation and abrogation of cell cycle checkpoints. Our results establish a central role for YAP in counteracting radiation-based therapies and driving genomic instability, and indicate the YAP/IGF2/Akt axis as a therapeutic target in medulloblastoma.

Introduction

Medulloblastoma, a primitive neuro-ectodermal tumor, is the most common malignant solid tumor of childhood. These tumors arise in the cerebellum, a brain structure that regulates posture and coordination, and develops largely peri-natally. Current medulloblastoma therapy entails surgery, radiation and chemotherapy. Over the past half century, the long-term survival rate for children with medulloblastoma has improved remarkably ranging from 40% to 70% after 5 years, yet recurrence is frequent and the overall mortality rate remains relatively high. Moreover, survivors suffer from serious long-term treatment-related

*Author for correspondence: Tel 615-936-3863 Fax 615-343-8104 Anna.Kenney@vanderbilt.edu.

Conflict of Interest The authors declare no conflict of interest.

sequelae. Current therapy combines surgery and chemotherapy with cranio-spinal irradiation. However, the long-term side effects of radiation therapy as well as the potential induction of secondary malignancies have inspired many investigators to find ways to reduce the amount of radiation used (Mueller and Chang 2009).

Medulloblastomas bearing evidence of Sonic hedgehog pathway activity, approximately 30% of cases (Northcott et al 2010), are proposed to arise from cerebellar granule neuron precursors (CGNPs) (Eberhart 2008). During cerebellar development, these cells undergo a rapid expansion phase, and their proliferation depends upon activation of the Sonic Hedgehog (Shh) signaling pathway (Dahmane and Ruiz i Altaba 1999, Wallace 1999, Wechsler-Reya and Scott 1999). Shh, a secreted ligand, signals by binding to the transmembrane protein Patched (Ptc), a tumor suppressor whose function is inhibit the activity of Smoothened, a transmembrane protein resembling a G protein-coupled receptor. In CGNPs, Shh interactions with Ptc relieve the inhibition of Smoothened and permit downstream signaling activity, resulting in activation of Gli, N-myc, and E2F1 transcription factors, and stabilization of insulin receptor substrate-1 (IRS1), all of which contribute to proliferation (Bhatia et al 2010, Kenney et al 2004, Oliver et al 2003, Parathath et al 2008, Ruiz i Altaba 1999). Loss of Patched or activating mutations in Smoothened are found in human medulloblastomas, and can be phenocopied in mice, through mutational inactivation of Ptc or transgenic expression of activating alleles of Smoothened (NeuroD2-SmoA1) in the cerebellum (Goodrich et al 1997, Hatton et al 2008). Recent observations in mouse models have demonstrated the importance of genome surveillance, as loss of DNA damage repair mechanisms can lead to genomic instability in neural progenitor cells, resulting in medulloblastoma, and can also cooperate with Shh signaling to enhance medulloblastoma formation in mice (Frappart et al 2009, Leonard et al 2008, Pazzaglia et al 2006, Tanori et al 2008).

Recently we have shown that Shh induces expression and activity of yes-associated protein (YAP), a transcriptional co-activator that is the target of the tumor suppressive Hippo pathway, and that YAP is highly expressed in Shh-associated medulloblastomas. YAP is known to have oncogenic properties, including the ability to promote epithelial-mesenchymal transition (EMT), suppression of apoptosis, growth factor-independent proliferation, and anchorage-independent growth in soft agar (Overholtzer et al 2006). YAP is involved in the formation of numerous tumors, including glioblastomas, oral squamous-cell carcinomas, and cancers of the pancreas, lung, ovary, and cervix (Fernandez and Kenney 2010, Zeng and Hong 2008, Zhao et al 2008). However, the effects exerted by YAP are highly context-dependent, as it acts as a tumor suppressor in other malignancies, such as some breast cancers (Yuan et al 2008). Similarly, YAP activity can have pro- or anti-apoptotic effects depending on the tissue and cell context (Bertini et al 2009).

Here, we show that YAP contributes to medulloblastoma growth and medulloblastoma cell survival after irradiation, through driving expression and production of Insulin-like Growth Factor 2 (IGF2) and subsequent activation of Akt. Akt activity endows tumor cells with the ability to evade the G1/S and G2/M checkpoints after irradiation, promoting their ongoing proliferation despite the presence of unrepaired DNA, thereby contributing to genomic instability. These novel findings reveal a link between oncogenic hedgehog signaling and

genomic instability, and they suggest that targeting YAP- and IGF-driven signaling pathways may have therapeutic value by restoring radiosensitivity and also permitting reduction of the radiation dose required to induce medulloblastoma tumor cell death.

Results

YAP expression promotes medulloblastoma cell tumorigenicity

We have previously shown that YAP is highly expressed in both human and mouse medulloblastomas, the YAP locus is highly amplified in 3% of the human medulloblastomas analyzed, and YAP expression is sufficient to drive proliferation of CGNPs in the absence of their obligate mitogen Shh (Fernandez et al 2009). In NeuroD2-SmoA1 mouse medulloblastomas, YAP is most highly expressed in tumor cells surrounding blood vessels, a micro-environment known as the peri-vascular niche (PVN). These cells are proposed to have “tumor repopulating” properties, and indeed, after irradiation these YAP-expressing cells can be found proliferating, possibly contributing to the regrowth of the tumor. To determine whether YAP expression increases medulloblastoma cell tumorigenicity, we cultured cells from medulloblastomas arising in NeuroD2-SmoA1 mice, infected them with retroviruses carrying either YAP or GFP, then implanted these cells intra-cranially into post-natal (PN) day 2 NOD/SCID pups. We then monitored the animals for symptomatic evidence of medulloblastoma (head tilt, seizures), confirmed upon sacrifice and dissection of the tumors. Ectopic expression of YAP enhances medulloblastoma growth, as determined by the ability of YAP-infected NeuroD2-SmoA1 cells to form tumors in the recipient mice, more effectively than GFP-infected NeuroD2 SmoA1 cells (14/17 YAP-SmoA1 injected mice vs. 8/17 GFP-SmoA1 injected mice). A similar trend was observed when wild-type C57BL/6 pups were used as recipients (Supplementary Figure 1). Moreover, YAP expression results in a significant acceleration of lethality (Long-rank Test, $p=0.0047$; Figure 1A; $p=0.0487$; Supplementary Figure 1), suggesting that YAP-expressing medulloblastomas are more aggressive. YAP-SmoA1 medulloblastomas have increased proliferation as determined by increased levels of cyclin D2 and phosphorylated Histone H3 (P-Hist3), markers of G1/S transition and mitosis phase of the cell cycle respectively (Figure 1B, C). YAP-SmoA1 tumors also showed reduced levels of apoptosis as determined by decreased levels of cleaved caspase 3 compared with tumors arising from GFP-infected SmoA1 cells. In keeping with our previous results, YAP is found throughout the tumor but is most highly expressed in PVN cells. Interestingly, YAP-expressing SmoA1 medulloblastomas also bear evidence of increased angiogenesis, suggested by higher levels of vascular endothelial growth factor (VEGF) and the endothelial cell marker CD31 (Figure 1B, C).

We have previously shown that YAP-expressing cells in Shh-induced mouse medulloblastomas proliferate after the animals have been treated with radiation. We next wished to determine whether YAP expression promotes survival after irradiation. To this end, we treated GFP-SmoA1 and YAP-SmoA1 medulloblastoma-bearing mice with 2 Gray (Gy) ionizing radiation and analyzed cell death and proliferation 3 hours post-irradiation. We observed a marked induction of cleaved caspase 3 in both tumors, but the levels of cleaved caspase 3 were less in YAP-SmoA1 tumors as compared to GFP-SmoA1 tumors

(Figure 1D). Moreover, irradiated YAP-SmoA1 medulloblastomas had significantly higher levels of P-Hist3 and Ki67 (Supplementary Figure 1B) in comparison with irradiated GFP-SmoA1 medulloblastomas. These lines of evidence indicate that YAP expression endows medulloblastoma cells with increased proliferation and survival capacities, and renders them radio-resistant.

YAP expression promotes increased proliferation, survival and cell cycle checkpoints override in irradiated cerebellar neural precursors

CGNPs are proposed to be the cell-of-origin for medulloblastomas associated with increased Shh pathway activity (Wechsler-Reya and Scott 1999). Consistent with this hypothesis, treatment of CGNPs in culture with exogenous Shh causes expression of many of the same proliferation markers seen in this class of medulloblastomas, including Gli1, N-myc and YAP. We wished to determine whether we could use *in vitro* primary CGNP cultures to mechanistically dissect the effects of YAP on proliferation and survival after irradiation. Cells prepared from post-natal day 4-5 mouse cerebella are maintained in serum free medium; addition of Shh sustains their proliferation. We transduced Shh-treated, proliferating CGNPs with retroviruses carrying GFP or YAP, then irradiated them (10 Gy) twenty-four hours later. As shown in Figure 2A, ectopic YAP expression is associated with increased CGNP proliferation as determined by cyclin D2 levels, and as we have previously reported (Fernandez et al 2009). At 20 hours post-irradiation, YAP-infected CGNPs had reduced levels of cleaved caspase 3 in comparison with GFP-infected CGNPs, and reduced numbers of apoptotic cells as determined by quantification of pyknotic nuclei (GFP: 62.5+/−0.5% vs YAP: 35.5+/−5.5%). YAP-transduced CGNPs were significantly more proliferative, as indicated by levels of cyclin D2, and by Ki67 and P-Hist3 staining (Figures 2A, B). Taken together, these results indicate that CGNP cultures recapitulate the *in vivo* effect of YAP expression on promoting survival and proliferation after irradiation. Moreover, they suggest that YAP-mediated radiation resistance may contribute to medulloblastoma recurrence by promoting increased tumor cell survival and proliferation.

Ionizing radiation (IR) causes the formation of double-strand DNA breaks (DSBs) that are responsible for the activation of the DNA Damage Response (DDR), a complex network of proteins required for cell-cycle checkpoint maintenance and DNA repair. The G1/S checkpoint prevents cells from entering S phase, while the G2/M checkpoint arrests cells with unrepaired DNA before entry into mitosis. We wanted to assess whether high YAP expression causes defects in cell cycle checkpoints, allowing cells to go through the cell cycle regardless of damage to their DNA. To examine the G1/S checkpoint, we exposed CGNPs to IR (10 Gy), and determined the percentage of cells in S phase 18 hours post-treatment by quantifying bromo-deoxyuridine (BrdU) incorporation during a one-hour pulse. Upon IR treatment both GFP and YAP-expressing CGNPs showed a strong reduction of the number of cells incorporating BrdU, however YAP-expressing cells have a significantly higher S-phase ratio (%BrdU-positive of treated/%BrdU-positive untreated), suggesting a mild defect in the G1/S checkpoint (Figure 2C). The infection efficiency was similar in both GFP- and YAP-infected cultures (representative images, Supplementary Figure 2). To determine whether the G2/M checkpoint was disabled in YAP-infected irradiated CGNPs, we evaluated P-Hist3 levels at an early time point (1 hour) after radiation. GFP-transduced

cells showed an 80% reduction of the number of P-Hist3 positive cells as compared to untreated cells. In contrast, YAP-expressing CGNPs showed only a 50% reduction of cells undergoing mitosis, indicating that the G2/M checkpoint was defective (Figure 2C).

YAP over-expression affects DNA repair and causes genomic instability

Defects in cell cycle checkpoints might result in genomic instability. We asked at which level YAP was affecting the DDR. Breaks in DNA are marked by the formation of protein complexes termed IR-induced foci (IRIF), which can be identified when analyzed by immunostaining for proteins comprising these complexes. To determine whether YAP-infected cells had reduced DNA damage, we carried out immunostaining for p53 binding protein 1 (53BP1), a key mediator of the DDR often used as a marker of the IRIF. At 3 hours post-irradiation, GFP- and YAP-infected CGNPs had similar numbers of foci per cell (data not shown). However, at 9 and 24 hours post-irradiation, YAP-infected CGNPs had a significantly reduced number of cells containing foci as well as fewer foci per cell (Figure 3A). These findings would suggest that YAP expression either enables cells to repair DNA more rapidly, causing foci to resolve earlier, or that YAP expression inhibits DNA repair pathways, resulting in dismantling of the DNA repair complexes.

To distinguish between these two possibilities, we carried out comet assays to detect broken DNA, in irradiated GFP- or YAP-infected CGNPs. In the comet assay, cells are immersed in an agarose matrix extended on a microscope slide, and treated with a lysis solution. Nuclear DNA is unwound under alkaline conditions and fragments resulting from strand breaks can migrate away from the nuclei under an electric field, forming a “comet tail” when stained. We quantified the amount of DNA damage by measuring tail lengths. As shown in Figure 3B, comet tails can be detected in GFP-infected CGNPs at 9 hours post-irradiation, but to a lesser extent at 24 hours post-irradiation, indicating that most of the damaged DNA is repaired at that point.

In contrast, at 9 hours after irradiation, YAP-infected cells had strikingly pronounced comet tails. Comet tails persisted in YAP-infected CGNPs 24 hours after irradiation, a time point at which we can detect proliferation in these cells (Figure 2). In order to analyze whether the DNA repair defect leads to chromosomal alterations, we performed metaphase spreads on GFP- or YAP-infected CGNPs 24 hours after irradiation. As shown in Figure 3C, YAP infection is associated with an increase in the number of cells with persistent DNA breaks. We also observed that YAP-transduced Pzp53^{med} cells (Berman et al 2002) showed a similar loss of irradiation-induced foci and increased number of cells with DNA breaks after irradiation (Supplementary Figure 3A, B). These observations indicate that YAP expression enables cells to proliferate with unrepaired DNA, a condition which can lead to genomic instability, a hallmark of cancer cells. To address whether the effect of YAP was specific for radiation-induced DNA damage, we treated GFP- and YAP-infected cells with the antibiotic Bleomycin, which causes double strand breaks in DNA. Similar to what we observed in irradiated cells, 9 and 24 hours after treatment there were significantly fewer cells that contained foci among those over-expressing YAP, which indicates that the role of YAP promoting focus dis-assembly is not specific to radiation-induced damage in the DNA (Supplementary Figure 3C).

YAP expression promotes inactivation of the checkpoint regulators ATM and Chk2

Entry into mitosis is marked by activation of the cyclin dependent kinase (Cdk)1: cyclin B1 complex. During G2, Cdk1 is maintained in an inactive state by phosphorylation on Thr 14 and Tyr 15 (Castedo et al 2002); de-phosphorylation by cdc25 disinhibits Cdk1. To confirm that YAP-expressing cells continued to enter mitosis after irradiation, indicating inactivation of the G2/M checkpoint, we carried out western blotting for Tyr 15-phosphorylated Cdk1. As shown in Figure 4A, irradiation results in increased Tyr15-phosphorylated Cdk1 in both GFP- and YAP-infected CGNPs. However, after three hours, YAP-infected CGNPs show reduced levels of Tyr15-phosphorylated Cdk1, indicating re-activation of Cdk1 at this early timepoint, when DNA breaks still persist. The reduction of inactive Cdk1 was associated with an increase in levels of cyclin B1, which is synthesized during interphase. Following metaphase, cyclin B1 is degraded; this degradation is required for completion of mitosis. Taken together, these results confirm that YAP-expressing irradiated CGNPs enter mitosis despite the presence of double-stranded DNA breaks, and they suggest that the G2/M arrest checkpoint is compromised by YAP expression.

These observations prompted us to examine whether YAP expression blocked activation of the G2/M checkpoint by affecting the activity of proteins involved in its regulation. Upon irradiation, the kinase ATM is activated by autophosphorylation and subsequently phosphorylates and activates Chk2 kinase. Chk2, in turn, phosphorylates cdc25c, resulting in its inactivation and preventing entry into mitosis (Reinhardt and Yaffe 2009). Irradiation resulted in increased levels of phosphorylated ATM and its substrate Chk2 in both GFP- and YAP-infected cells. However, in the presence of ectopic YAP, ATM and Chk2 were more rapidly dephosphorylated (Figure 4B, western blot with quantification below). We observed a similar trend towards Chk2 inactivation in medulloblastoma cells (MBC) obtained from SmoA1 medulloblastomas, cultured *in vitro* and transduced with either GFP or YAP. Our observation of ATM and Chk2 inactivation in YAP-infected CGNPs and MBC is consistent with relief from the G2/M checkpoint and consequently, re-entry into mitosis despite the presence of unrepaired DNA breaks. We also observed reduced phosphorylation of Histone H2AX in YAP-transduced irradiated CGNPs, further indicative of impaired DNA damage response pathway signaling (Supplementary Figure 4A). Interestingly, we did not observe differential effects of YAP expression on regulation of Chk1 or p53 activity after exposure to radiation in CGNPs or MBC, indicating that YAP's downstream effectors preferentially target the ATM/Chk2 DNA damage response pathway (Figure 4B).

IGF2 is a candidate YAP target mediating proliferation and survival after irradiation

We next wished to gain insight as to the mechanism through which YAP protects tumor cells from radiation-induced apoptosis and allows them to continue cycling. YAP functions in a complex with TEAD to regulate gene expression and proliferation (Zhao et al 2008). To determine which genes may be induced or suppressed by YAP in irradiated CGNPs, we carried out microarray analysis of mRNA prepared from GFP- or YAP-infected control or irradiated CGNPs. Among the genes most highly expressed in YAP-infected CGNPs was IGF2, confirmed by quantitative RT-PCR (Figure 5A). IGF2 mRNA expression was increased in both cell populations after irradiation, but the levels of IGF2 in the YAP-infected CGNPs were significantly higher than in the GFP-infected cell under either

condition (non-irradiated or irradiated). When we analyzed IGF2 protein levels in GFP- or YAP-infected CGNPs we found that YAP-infected CGNPs expressed and secreted significantly more IGF2 (Figures 5B, C).

IGF signaling is required for survival of CGNPs *in vivo* and *in vitro*, and increased activity of the IGF pathway is found in human medulloblastomas (Chrysis et al 2001, Corcoran et al 2008, Hahn et al 2000, Hartmann et al 2005, Rao et al 2004, Tanori et al 2010). Interestingly, when we queried a genetically characterized database of over 100 human medulloblastomas (Northcott et al 2009b) we found that *IGF2* was most highly expressed in the subclass of medulloblastomas associated with activation of the Shh pathway (T test, p=3.553E-14) (Figure 5D). This class of tumors also expresses high levels of *N-myc*, *Gli1*, and *miR17/92* (Kool et al 2008, Northcott et al 2009b, Pomeroy et al 2002). The increased level of IGF2 protein in YAP-expressing tumors was conserved in YAP-SmoA1 medulloblastomas, as determined by western blot and immunohistochemical analysis (Figure 5E, F). As we observed in CGNPs, IGF2 levels are increased in both GFP-SmoA1 and YAP-SmoA1 medulloblastomas after irradiation, but are higher in YAP-SmoA1 medulloblastomas.

IGF2 acts as a secreted ligand, binding to and activating the IGF1 receptor. The predominant downstream effector of the activated IGF1 receptor is the kinase Akt, which plays multiple roles in survival and proliferation. We have previously shown that Akt cooperates with Shh signaling to promote proliferation through stabilization of N-myc (Kenney et al 2004). Akt activity has been linked to abrogation of the G2/M checkpoint after irradiation, through inactivation of ATM/Chk2 (Hirose et al 2005, Kandel et al 2002). Consistent with increased IGF1 receptor activity in response to IGF2 secretion, YAP-Smo-driven medulloblastomas exhibit higher levels of activated Akt (S473-phosphorylated), most notably in cells surrounding the vasculature (Figure 5G); interestingly, these cells also express the highest levels of YAP and they have been proposed to function as tumor repopulating cells after irradiation (Fernandez et al 2009, Hambardzumyan et al 2008). Taken together these observations raise the possibility that YAP-mediated IGF2 induction not only promotes survival and proliferation through Akt activation but may also affect the phosphorylation of ATM/Chk2, resulting in disruption of the G2/M checkpoint.

IGF2 is required for YAP-mediated G2/M arrest override and cell survival and proliferation after irradiation

To address whether IGF2/Akt activity regulates the YAP-associated DNA damage response defect after radiation, we used Shh-treated CGNP cultures. Confirming our observations (Figure 5), YAP infection is associated with increased Akt activity (Figure 6A) as determined by phosphorylation of S473. Treatment of YAP-infected CGNPs with the drug LY294002, which inhibits phosphoinositide-3 kinase, the upstream activator of Akt, reduced levels of S473-phosphorylated Akt. After irradiation, we saw induction of ATM phosphorylation in GFP- and YAP-infected CGNPs, although to a lesser extent in the presence of ectopic YAP, indicating reduced activity of this kinase. In keeping with reduced ATM activity in the presence of YAP, we also observed reduced Chk2 phosphorylation. In

the presence of LY294002, full ATM and Chk2 phosphorylation were recovered, indicating that YAP requires Akt activity for its suppressive effect on ATM and Chk2.

We next wished to determine whether IGF2 is necessary for the effects of YAP on the DNA damage response. To this end, we used retroviruses targeting IGF2 for short hairpinRNA-mediated knock-down. As shown in Figure 6B, YAP-infected CGNPs transduced with these retroviruses showed strikingly reduced levels of IGF2, in comparison with YAP-infected CGNPs transduced with retroviruses carrying a scrambled, non-specific short hairpin RNA sequence. Consistent with IGF2 being an upstream activator of Akt, IGF2 knockdown was associated with reduced Akt Ser473 phosphorylation. In addition, knocking down IGF2 in YAP-expressing cells led to a recovery of phospho-ATM and phospho-Chk2 levels, as well as phospho-Cdk1, comparable to those observed in GFP-infected cells. The increase in inactive Cdk1 when IGF2 is knocked down indicates cells arresting after radiation, due to a restored G2/M checkpoint. IGF2 knock-down also blocked the effects of YAP on DNA damage-dependent focus formation after irradiation (Figure 6C), causing a significant rescue of focus formation as determined by immunofluorescent staining for 53BP1. Moreover, IGF2 knock-down impaired the effects of YAP expression on CGNP survival after irradiation, as well as proliferation (Figure 6D). These results are consistent with IGF2 and its downstream effector Akt being necessary for the ability of YAP to inactivate the G2/M checkpoint, permitting ongoing proliferation and enhancing survival of irradiated cells.

Discussion

Amplification of the *YAP* gene locus as well as YAP protein over-expression has been reported in a wide spectrum of human and murine tumors. We have previously shown that YAP is a downstream target of mitogenic Sonic hedgehog signaling that promotes proliferation and inhibits apoptosis of cerebellar granule cell precursors and we showed that YAP is over-expressed and amplified in the Sonic hedgehog-associated class of medulloblastomas (Fernandez et al 2009). Here, we report a new role for YAP in promoting IGF2/Akt-dependent radio-resistance and ongoing proliferation in the presence of unrepaired DNA, illustrating a novel link between Shh signaling, YAP, and the Akt pathway. We show that YAP activity markedly induces IGF2 transcription, in the absence and presence of radiation. IGF2, in turn, activates Akt downstream of PI-3 kinase, providing cells with a survival and proliferative advantage, and allowing them to inactivate cell cycle checkpoints (Figure 7). Many studies have implicated PI-3 kinase and Akt in cell survival, through its effects on FKHR proteins and Bcl2 family members (Brunet et al 2001, Burgering and Kops 2002, Duronio 2008), and Akt is essential for CGNP survival (Dudek et al 1997). Transcriptional profiling of human medulloblastomas has shown increased expression of IGF2 (Pomeroy et al 2002), and our report clearly links high levels of IGF2 expression with the Sonic hedgehog-associated subclass of medulloblastomas. IGF2 has been shown to be indispensable for the formation and progression of Shh-driven murine medulloblastomas (Corcoran et al 2008, Hahn et al 2000) and to synergize with Sonic Hedgehog in the induction of tumor formation (Rao et al 2004). IGF2 has previously been shown to promote proliferation of medulloblastoma cells and cerebellar neural cell precursors through the activation of Akt (Hartmann et al 2005).

Our results show that ectopic YAP expression accelerates medulloblastoma onset and aggressiveness, and also confers a survival advantage after tumor radiation. This has particularly important implications for medulloblastomas; due to their radiosensitivity, radiation therapy is a standard in children older than 3 years of age (Mueller and Chang 2009). We show here that 3 hours after radiation, YAP-driven SmoA1 medulloblastomas feature higher levels of proliferation markers and reduced apoptosis. *In vitro*, we found a similar effect when we irradiated GFP- or YAP-over-expressing CGNPs. CGNPs expressing YAP not only proliferated more than GFP-expressing cells after radiation, but also failed to arrest in response to radiation, skipping the G2/M checkpoint.

Defective G2/M checkpoint activation in the presence of DNA damage has been linked to Akt activity. Activation of Akt suppresses the checkpoint by inhibiting the DNA damage response pathways, either ATM/Chk2 or ATR/Chk1, depending on the cellular context (Hirose et al 2005, Kandel et al 2002, Shtivelman et al 2002, Xu et al 2010). In agreement with these studies, we observed a decrease in phosphorylated ATM and Chk2 in irradiated YAP-over-expressing CGNPs and medulloblastoma cells, compared to GFP-expressing cells, and YAP-transduced cells showed fewer DNA damage-induced foci. The effects of YAP on ATM and Chk2 was reversed in the presence of a PI-3 kinase inhibitor, and when we knocked down IGF2, which also abolished the accelerating effect of YAP on DNA damage-dependent focus disassembly. Interestingly, a previous study has shown that aberrant activation of the Shh pathway through Ptc loss-of-function impairs the function of ATR/Chk1, a separate signaling cascade (Leonard et al 2008). We did not detect effects of YAP on this cascade (data not shown); however the impact we report of YAP on ATM/Chk2 may synergize with an already defective DNA damage response due to Smoothened-mediated Chk1 impairment.

The ability of cells to maintain genomic integrity is fundamental for protection from cancer development. Genomic instability characterizes almost all sporadic human cancers, although mechanisms causing it are still not well understood. High-throughput sequencing studies suggest that mutations in DNA repair genes do not account for the presence of genomic instability in many sporadic cancers (Negrini et al 2010). Alternatively, activation of oncogenes, and more generally of growth signaling pathways, has been shown to induce genomic instability in mammalian cells cultured *in vitro* and in mouse models (Hernando et al 2004, Negrini et al 2010). Hyperactive Shh pathway activity has been shown to induce genomic instability and the development of spontaneous and ionizing radiation (IR)-induced tumors (Leonard et al 2008). Now we show that high levels of YAP expression further contribute to generation of genomic instability since irradiated YAP-expressing cells present a higher number of chromosomal alterations. The role of genomic instability has remained a controversial issue in cancer biology. Although it is still unclear if it is necessary for tumorigenesis to occur, genomic instability certainly provides the tumor with an advantage in terms of faster progression through the many stages of tumorigenesis (Sieber et al 2003). Indeed, we show that ectopic expression of YAP accelerates medulloblastoma onset and produces tumors that are highly aggressive and rapidly lethal.

YAP expression is particularly high in the peri-vascular niche (PVN) of medulloblastomas, where the tumor-repopulating cells reside. We have previously shown that 48 hours after

radiation, the YAP positive population starts to expand (Fernandez et al 2009). Hambardzumyan et al. (Hambardzumyan et al 2008) elegantly demonstrated that the PI3K-Akt pathway regulates survival of these tumor-repopulating cells residing in the PVN. These results point to the importance of YAP regulating survival and proliferation post-radiation, allowing the cells to skip the cell cycle checkpoints and expand despite the un-repaired damage in their DNA, contributing ultimately to genomic instability. Further studies will address whether YAP-induced genomic instability is solely a consequence of the Akt-mediated cell cycle checkpoint suppression, or whether Akt lying downstream of YAP-induced IGF2 could also inhibit the DNA repair machinery, as previous studies have suggested (Plo et al 2008) (Figure 7). Our results suggest that targeting Akt downstream of YAP would be useful for medulloblastoma therapy in order to reduce the dose of radiation needed and to prevent tumor recurrence, by radiosensitizing PVN-residing tumor-repopulating cells.

Materials and Methods

Animal studies

Harvest of cerebellar granule neuron precursors from neonatal mice, preparation of cerebella and tumor tissue from wild-type and mutant mice for histological analysis, and irradiation of tumor-bearing mice were carried out in compliance with the Memorial Sloan-Kettering Institutional animal care and use committee guidelines. *NeuroD2-SmoA1* mice were provided by Jim Olson (Fred Hutchinson Cancer Research Center). *Patched*$^{+/-}$ mice were provided by Kathryn Anderson (Memorial Sloan-Kettering Cancer Center). NOD/SCID mice were purchased from The Jackson Laboratory.

Human tumor collection and expression analysis

Exon array profiling and data analysis with tumor sub-grouping were performed as published (Northcott et al 2009a).

CGNPs and medulloblastoma cell culture

CGNP cultures were generated as previously described (Kenney and Rowitch 2000). Cells were plated on individual poly-DL-ornithine (Sigma) pre-coated plates or pre-coated glass coverslips. In all cases cells were treated with 3 μg/mL of Shh. Where indicated, LY 294002 (Sigma) was used at a concentration of 10 nM for 6h.

Medulloblastoma cells (MBC) were obtained from SmoA1 mouse medulloblastomas. Briefly, tumors were disassociated and cells were incubated in Trypsin/EDTA solution for 30 minutes, then passed through a cell strainer. Cells were subsequently separated on a density step gradient of 35% and 60% Percoll solution (Sigma). Purified MBCs were enriched by pre-plating on uncoated tissue culture dishes to remove adherent fibroblasts and glial cells. Non-adherent cells were plated on tissue culture dishes pre-coated with poly D-lysine (Sigma) and Matrigel (BD Biosciences), infected with retroviruses 24 hours later, and cultured for 24 more hours before implantation or irradiation.

Tumor cell implantation

0.2 million MBC were injected in the cortices of P2 NOD/SCID or C57BL/6 pups with a stereotaxic syringe.

Retrovirus production and infection

The YAP cassette was cloned from pBabe-YAP1 (Addgene) into the retroviral vector pWzl. Short hairpin RNA interference sequences targeting IGF2 at the 3′ or 5′ end of the coding sequence were designed using the Cold Spring Harbor Laboratory RNAi OligoRetriever database and ligated into pSHAG vector, then transferred to MSCV retroviral vector and produced as described (Nahle et al 2008). A control scrambled shRNA retrovirus was also prepared. 293 EBNA (Invitrogen) packaging cells were co-transfected with gag-pol and VSVg packaging plasmids plus pWzl-eGFP, pWzl-YAP1, pMSCV-IGF2shRNA or a control scrambled shRNA using Fugene 6 transfection reagent (Roche). The media was changed 12 hours after transfection and supernatants (8 mL) were harvested at 24 and 48 hours and filtered through 0.45 μm syringe filters. For infection, Shh-treated CGNPs were exposed to the viral supernatants for 3 hours. Viral supernatant was then removed and replaced with fresh medium + Shh.

RNA extraction and Real Time PCR

Total RNA from cerebellar granule neural precursors was extracted and purified using the MiRvana kit (Ambion). cDNA was prepared from 1 μg total RNA by using iScript cDNA Synthesis kit (Bio-Rad). qPCR was performed using TaqMan Universal PCR Master Mix (Applied Biosystems). RNA expression data were acquired and analysed using an StepOnePlus Real Time PCR system (Applied Biosystems). Average results and standard errors are presented. TaqMan probes used for qPCR were IGF2 (Mm01163433-m1) and control HPRT1 (Mm01545399-m1).

Protein preparation and immunoblotting

Protein extracts were prepared as previously described (Kenney and Rowitch, 2000). Protein content was determined by using the Bio-Rad protein assay. 50-75 μg of each sample was separated by sodium dodecyl sulfate-polyacrylamide gel electrophoresis (SDS-PAGE) on 8-10% polyacrylamide gels and then transferred in 20% methanol buffer at 4°C to Immobilon polyvinylidene difluoride (Millipore) membranes. Immunoblotting was carried out according to standard methods. Antibodies used for western blotting were: YAP1 (Abcam), phospho-Akt (Ser473), phospho-Cdk1(Tyr15), phospho-Chk2 (Thr68), total Akt and cleaved caspase 3 (Cell Signaling), phospho-ATM (Ser1981) (Rockland), Chk2 (Millipore), IGF2 and β-tubulin (Sigma), VEGF, Cyclin D2 and Cyclin B1 (Santa Cruz). Donkey anti-mouse HRP-linked secondary was from Jackson Research Laboratories and goat anti-rabbit from Thermo Scientific. Peroxidase activity was detected using Amershams's ECL reagents and exposing membranes to Kodak Biomax film.

Cell and tissue immunostaining

For immunofluorescence 8μm sections of paraformaldehyde-fixed/paraffin-embedded tissues were first de-waxed and re-hydrated prior to antigen retrieval. CGNPs were cultured

on poly-DL-ornithine coated glass coverslips as previously described. Cells were fixed with 4% paraformaldehyde for 20 minutes. Immunofluorescent staining of sections and cells was carried out according to standard methods. Immunohistochemical staining was performed using a Discovery XT automated staining processor (Ventana Medical Systems, Inc.). Antibodies used were: Ki67 (Vector Labs), YAP1 (Abcam), CD31 (BD Transduction Laboratories), GFP (Invitrogene), BrdU (BD Biosciences), p53BP1 and IGF2 (Novus Biologicals), phospho-histone 3, cleaved caspase 3 and phospho-Akt(Ser473) (Cell Signaling).

Image capturing

Staining of cultured primary cells and tissue sections was visualized with a Leica DM5000B microscope and images were taken using Leica FW400 software. For quantification, TIFF images of 5-10 random fields were taken for each experimental group and average pixel intensities were measured using Image J and Volocity softwares.

Mitosis spreads

Metaphase preparations were done by the Molecular Cytogenetics core facility at Memorial Sloan-Kettering Cancer Center according to standard procedures.

Comet Assay

The comet assay was performed with the Trevigen kit and following the manufacturer's instructions. Tail lengths were calculated using Comet Assay IV software. Averages from four independent experiments were calculated and representative pictures are shown.

ELISA

Supernatants from CGNPs infected with GFP or YAP and subsequently cultured in 800 μL minimal media without N2 supplement were collected. IGF2 ELISA was performed using the R&D systems kit and following the manufacture's instructions. Triplicates were used in each case and the average from three independent experiments is shown.

Supplementary Material

Refer to Web version on PubMed Central for supplementary material.

Acknowledgements

We are grateful to Martine Roussel and her group at St. Jude Children's Research Hospital for training and advice on medulloblastoma cell culture and intracranial implantation. AF-L received support from the Spanish Ministry of Education, the Charles H. Revson Foundation, and the Childhood Brain Tumor Foundation. This work was supported by grants to AMK from the Alex's Lemonade Stand Foundation, National Brain Tumor Society, James S. McDonnell Foundation, and the NIH (NINDS R01NS061070).

REFERENCES

Berman DM, Karhadkar SS, Hallahan AR, Pritchard JI, Eberhart CG, Watkins DN, et al. Medulloblastoma growth inhibition by hedgehog pathway blockade. Science. 2002; 297:1559–1561. [PubMed: 12202832]

Bertini E, Oka T, Sudol M, Strano S, Blandino G. YAP: at the crossroad between transformation and tumor suppression. Cell Cycle. 2009; 8:49–57. [PubMed: 19106601]

Bhatia B, Hsieh M, Kenney AM, Nahle Z. Mitogenic Sonic hedgehog signaling drives E2F1-dependent lipogenesis in progenitor cells and medulloblastoma. Oncogene. 2010

Brunet A, Datta SR, Greenberg ME. Transcription-dependent and - independent control of neuronal survival by the PI3K-Akt signaling pathway. Curr Opin Neurobiol. 2001; 11:297–305. [PubMed: 11399427]

Burgering BM, Kops GJ. Cell cycle and death control: long live Forkheads. Trends Biochem Sci. 2002; 27:352–360. [PubMed: 12114024]

Castedo M, Roumier T, Blanco J, Ferri KF, Barretina J, Tintignac LA, et al. Sequential involvement of Cdk1, mTOR and p53 in apoptosis induced by the HIV-1 envelope. EMBO J. 2002; 21:4070–4080. [PubMed: 12145207]

Chrysis DC, Alexandrides TK, Koromantzou E, Georgopoulos N, Vassilakos P, Kiess W, et al. Novel application of IGF-I and IGFBP-3 generation tests in the diagnosis of growth hormone axis disturbances in children with beta-thalassaemia. Clin Endocrinol (Oxf). 2001; 54:253–259. [PubMed: 11207641]

Corcoran RB, Raveh T Bachar, Barakat MT, Lee EY, Scott MP. Insulin-like growth factor 2 is required for progression to advanced medulloblastoma in patched1 heterozygous mice. Cancer Res. 2008; 68:8788–8795. [PubMed: 18974121]

Dahmane N, Ruiz i Altaba A. Sonic hedgehog regulates the growth and patterning of the cerebellum. Development. 1999; 126:3089–3100. [PubMed: 10375501]

Dudek H, Datta SR, Franke TF, Birnbaum MJ, Yao R, Cooper GM, et al. Regulation of neuronal survival by the serine-threonine protein kinase Akt. Science. 1997; 275:661–665. [PubMed: 9005851]

Duronio V. The life of a cell: apoptosis regulation by the PI3K/PKB pathway. Biochem J. 2008; 415:333–344. [PubMed: 18842113]

Eberhart CG. Even cancers want commitment: lineage identity and medulloblastoma formation. Cancer Cell. 2008; 14:105–107. [PubMed: 18691544]

Fernandez LA, Northcott PA, Dalton J, Fraga C, Ellison D, Angers S, et al. YAP1 is amplified and up-regulated in hedgehog-associated medulloblastomas and mediates Sonic hedgehog-driven neural precursor proliferation. Genes Dev. 2009; 23:2729–2741. [PubMed: 19952108]

Fernandez LA, Kenney AM. The Hippo in the room: A new look at a key pathway in cell growth and transformation. Cell Cycle. 2010; 9

Frappart PO, Lee Y, Russell HR, Chalhoub N, Wang YD, Orii KE, et al. Recurrent genomic alterations characterize medulloblastoma arising from DNA double-strand break repair deficiency. Proc Natl Acad Sci U S A. 2009; 106:1880–1885. [PubMed: 19164512]

Goodrich LV, Milenkovic L, Higgins KM, Scott MP. Altered neural cell fates and medulloblastoma in mouse patched mutants. Science. 1997; 277:1109–1113. [PubMed: 9262482]

Hahn H, Wojnowski L, Specht K, Kappler R, Calzada-Wack J, Potter D, et al. Patched target Igf2 is indispensable for the formation of medulloblastoma and rhabdomyosarcoma. J Biol Chem. 2000; 275:28341–28344. [PubMed: 10884376]

Hambardzumyan D, Becher OJ, Rosenblum MK, Pandolfi PP, Manova-Todorova K, Holland EC. PI3K pathway regulates survival of cancer stem cells residing in the perivascular niche following radiation in medulloblastoma in vivo. Genes Dev. 2008; 22:436–448. [PubMed: 18281460]

Hartmann W, Koch A, Brune H, Waha A, Schuller U, Dani I, et al. Insulin-like growth factor II is involved in the proliferation control of medulloblastoma and its cerebellar precursor cells. Am J Pathol. 2005; 166:1153–1162. [PubMed: 15793295]

Hatton BA, Villavicencio EH, Tsuchiya KD, Pritchard JI, Ditzler S, Pullar B, et al. The Smo/Smo model: hedgehog-induced medulloblastoma with 90% incidence and leptomeningeal spread. Cancer Res. 2008; 68:1768–1776. [PubMed: 18339857]

Hernando E, Nahle Z, Juan G, Diaz-Rodriguez E, Alaminos M, Hemann M, et al. Rb inactivation promotes genomic instability by uncoupling cell cycle progression from mitotic control. Nature. 2004; 430:797–802. [PubMed: 15306814]

Hirose Y, Katayama M, Mirzoeva OK, Berger MS, Pieper RO. Akt activation suppresses Chk2-mediated, methylating agent-induced G2 arrest and protects from temozolomide-induced mitotic catastrophe and cellular senescence. Cancer Res. 2005; 65:4861–4869. [PubMed: 15930307]

Kandel ES, Skeen J, Majewski N, Di Cristofano A, Pandolfi PP, Feliciano CS, et al. Activation of Akt/protein kinase B overcomes a G(2)/m cell cycle checkpoint induced by DNA damage. Mol Cell Biol. 2002; 22:7831–7841. [PubMed: 12391152]

Kenney AM, Rowitch DH. Sonic hedgehog promotes G(1) cyclin expression and sustained cell cycle progression in mammalian neuronal precursors. Mol Cell Biol. 2000; 20:9055–9067. [PubMed: 11074003]

Kenney AM, Widlund HR, Rowitch DH. Hedgehog and PI-3 kinase signaling converge on Nmyc1 to promote cell cycle progression in cerebellar neuronal precursors. Development. 2004; 131:217–228. [PubMed: 14660435]

Kool M, Koster J, Bunt J, Hasselt NE, Lakeman A, van Sluis P, et al. Integrated genomics identifies five medulloblastoma subtypes with distinct genetic profiles, pathway signatures and clinicopathological features. PLoS ONE. 2008; 3:e3088. [PubMed: 18769486]

Leonard JM, Ye H, Wetmore C, Karnitz LM. Sonic Hedgehog signaling impairs ionizing radiation-induced checkpoint activation and induces genomic instability. J Cell Biol. 2008; 183:385–391. [PubMed: 18955550]

Mueller S, Chang S. Pediatric brain tumors: current treatment strategies and future therapeutic approaches. Neurotherapeutics. 2009; 6:570–586. [PubMed: 19560746]

Nahle Z, Hsieh M, Pietka T, Coburn CT, Grimaldi PA, Zhang MQ, et al. CD36-dependent regulation of muscle FoxO1 and PDK4 in the PPAR delta/beta-mediated adaptation to metabolic stress. J Biol Chem. 2008; 283:14317–14326. [PubMed: 18308721]

Negrini S, Gorgoulis VG, Halazonetis TD. Genomic instability--an evolving hallmark of cancer. Nat Rev Mol Cell Biol. 2010; 11:220–228. [PubMed: 20177397]

Northcott PA, Fernandez LA, Hagan JP, Ellison DW, Grajkowska W, Gillespie Y, et al. The miR-17/92 polycistron is up-regulated in sonic hedgehog-driven medulloblastomas and induced by N-myc in sonic hedgehog-treated cerebellar neural precursors. Cancer Res. 2009a; 69:3249–3255. [PubMed: 19351822]

Northcott PA, Nakahara Y, Wu X, Feuk L, Ellison DW, Croul S, et al. Multiple recurrent genetic events converge on control of histone lysine methylation in medulloblastoma. Nat Genet. 2009b; 41:465–472. [PubMed: 19270706]

Northcott PA, Korshunov A, Witt H, Hielscher T, Eberhart CG, Mack S, et al. Medulloblastoma Comprises Four Distinct Molecular Variants. J Clin Oncol. 2010

Oliver TG, Grasfeder LL, Carroll AL, Kaiser C, Gillingham CL, Lin SM, et al. Transcriptional profiling of the Sonic hedgehog response: a critical role for N-myc in proliferation of neuronal precursors. Proc Natl Acad Sci U S A. 2003; 100:7331–7336. [PubMed: 12777630]

Overholtzer M, Zhang J, Smolen GA, Muir B, Li W, Sgroi DC, et al. Transforming properties of YAP, a candidate oncogene on the chromosome 11q22 amplicon. Proc Natl Acad Sci U S A. 2006; 103:12405–12410. [PubMed: 16894141]

Parathath SR, Mainwaring LA, Fernandez LA, Campbell DO, Kenney AM. Insulin receptor substrate 1 is an effector of sonic hedgehog mitogenic signaling in cerebellar neural precursors. Development. 2008; 135:3291–3300. [PubMed: 18755774]

Pazzaglia S, Tanori M, Mancuso M, Rebessi S, Leonardi S, Di Majo V, et al. Linking DNA damage to medulloblastoma tumorigenesis in patched heterozygous knockout mice. Oncogene. 2006; 25:1165–1173. [PubMed: 16407852]

Plo I, Laulier C, Gauthier L, Lebrun F, Calvo F, Lopez BS. AKT1 inhibits homologous recombination by inducing cytoplasmic retention of BRCA1 and RAD51. Cancer Res. 2008; 68:9404–9412. [PubMed: 19010915]

Pomeroy SL, Tamayo P, Gaasenbeek M, Sturla LM, Angelo M, McLaughlin ME, et al. Prediction of central nervous system embryonal tumour outcome based on gene expression. Nature. 2002; 415:436–442. [PubMed: 11807556]

Rao G, Pedone CA, Del Valle L, Reiss K, Holland EC, Fults DW. Sonic hedgehog and insulin-like growth factor signaling synergize to induce medulloblastoma formation from nestin-expressing neural progenitors in mice. Oncogene. 2004; 23:6156–6162. [PubMed: 15195141]

Reinhardt HC, Yaffe MB. Kinases that control the cell cycle in response to DNA damage: Chk1, Chk2, and MK2. Curr Opin Cell Biol. 2009; 21:245–255. [PubMed: 19230643]

Ruiz i Altaba A. Gli proteins encode context-dependent positive and negative functions: implications for development and disease. Development. 1999; 126:3205–3216. [PubMed: 10375510]

Shtivelman E, Sussman J, Stokoe D. A role for PI 3-kinase and PKB activity in the G2/M phase of the cell cycle. Curr Biol. 2002; 12:919–924. [PubMed: 12062056]

Sieber OM, Heinimann K, Tomlinson IP. Genomic instability--the engine of tumorigenesis? Nat Rev Cancer. 2003; 3:701–708. [PubMed: 12951589]

Tanori M, Mancuso M, Pasquali E, Leonardi S, Rebessi S, Di Majo V, et al. PARP-1 cooperates with Ptc1 to suppress medulloblastoma and basal cell carcinoma. Carcinogenesis. 2008; 29:1911–1919. [PubMed: 18660545]

Tanori M, Santone M, Mancuso M, Pasquali E, Leonardi S, Di Majo V, et al. Developmental and oncogenic effects of insulin-like growth factor-I in Ptc1+/− mouse cerebellum. Mol Cancer. 2010; 9:53. [PubMed: 20214787]

Wallace VA. Purkinje-cell-derived Sonic hedgehog regulates granule neuron precursor cell proliferation in the developing mouse cerebellum. Curr Biol. 1999; 9:445–448. [PubMed: 10226030]

Wechsler-Reya RJ, Scott MP. Control of neuronal precursor proliferation in the cerebellum by Sonic Hedgehog. Neuron. 1999; 22:103–114. [PubMed: 10027293]

Xu N, Hegarat N, Black EJ, Scott MT, Hochegger H, Gillespie DA. Akt/PKB suppresses DNA damage processing and checkpoint activation in late G2. J Cell Biol. 2010; 190:297–305. [PubMed: 20679434]

Yuan M, Tomlinson V, Lara R, Holliday D, Chelala C, Harada T, et al. Yes-associated protein (YAP) functions as a tumor suppressor in breast. Cell Death Differ. 2008; 15:1752–1759. [PubMed: 18617895]

Zeng Q, Hong W. The emerging role of the hippo pathway in cell contact inhibition, organ size control, and cancer development in mammals. Cancer Cell. 2008; 13:188–192. [PubMed: 18328423]

Zhao B, Ye X, Yu J, Li L, Li W, Li S, et al. TEAD mediates YAP-dependent gene induction and growth control. Genes Dev. 2008; 22:1962–1971. [PubMed: 18579750]

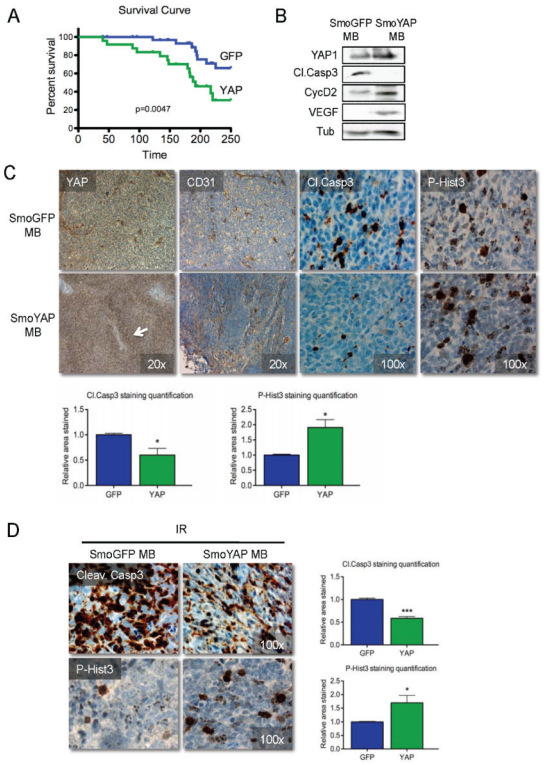

Figure 1. YAP promotes medulloblastoma cell tumorigenicity, proliferation and survival

(A) Tumor-free survival curve. Two hundred thousand NeuroD2-SmoA1 tumor cells transduced with either GFP or YAP were implanted into the brain of NOD/SCID post-natal day 2 pups. Animals were sacrificed when they developed symptoms. YAP-over-expressing medulloblastomas occurred with a higher penetrance and earlier development compared to GFP-transduced tumors (Long-rank Test, p=0.0047). 14/17 animals implanted with YAP-SmoA1 medulloblastomas cells developed tumors while only 8/17 animals implanted with GFP-SmoA1 cells did. A similar trend was observed when nonimmunocompromised recipient pups were used (Long-rank Test, p=0.0487; Supplementary Figure 1).

(B) Representative western blot analysis of GFP-SmoA1 and YAP-SmoA1 medulloblastomas. Note reduced cleaved caspase 3, increased cyclin D2, and increased VEGF in YAP-SmoA1 medulloblastoma.

(C) Immunohistochemical analysis of YAP, the endothelial cell marker CD31, cleaved caspase 3, and phosphorylated histone H3 in GFP-SmoA1 (top) and YAP-SmoA1 (bottom) medulloblastomas. YAP-SmoA1 tumors have significantly reduced apoptosis and increased proliferation compared with GFP-SmoA1 tumors, indicated in the graphs.

(D) Immunohistochemical analysis and quantification of apoptosis (cleaved caspase 3) and proliferation (phosphorylated histone H3) in GFP-SmoA1 and YAP-SmoA1 medulloblastomas three hours after tumor-bearing animals were irradiated (2 Gy). Statistically significant differences are indicated as (*) $P < 0.05$; (***) $P < 0.001$.

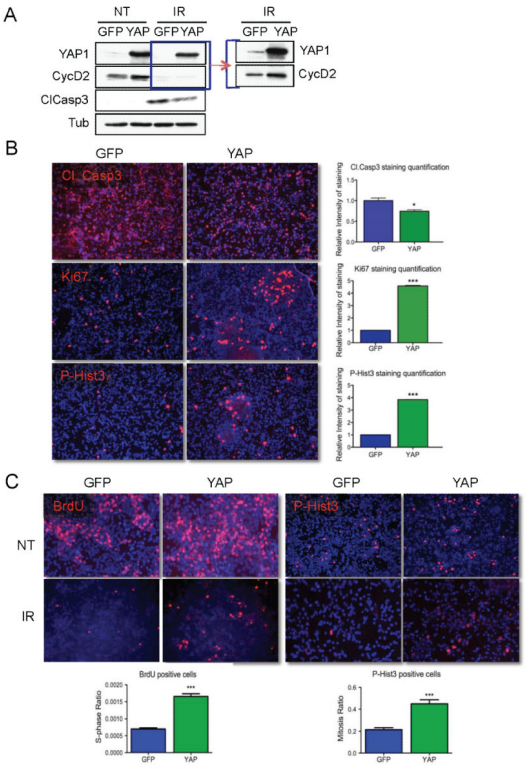

Figure 2. YAP promotes proliferation and survival in irradiated CGNPs

(A) Western blot analysis of proliferation (cyclin D2) and apoptosis (cleaved caspase 3) in GFP- or YAP-transduced Shh-treated CGNPs untreated (NT) and 20 hours after γ-irradiation (IR) with 10 Gy. Panel to the right shows over-exposed image. Similar infection efficiencies were obtained with both retroviruses (Supplementary Figure 2).

(B) Immunofluorescence analysis and quantification of cleaved caspase 3 and the proliferation markers Ki67 and phosphorylated histone H3 (P-Hist3) in GFP- or YAP-transduced CGNPs 20 hours post-irradiation.

(C) Left, immunofluorescence analysis of BrdU incorporation (1-hour pulse) untreated (NT; top panels) and 18 hours after irradiation (IR; middle panels). The S-phase ratios for GFP and YAP-transduced CGNPs (%BrdU-positive of treated / %BrdU-positive untreated) are shown at the bottom. Irradiated GFP-transduced cells were normalized to non-irradiated GFP-transduced CGNPs; irradiated YAP-transduced CGNPs were normalized to non-irradiated YAP-transduced CGNPs. The higher S-phase ratio indicates that YAP-over-expressing CGNPs present a defect in the G1/S checkpoint. Right, immunofluorescence analysis of phosphorylated histone H3 before (NT; top panels) and 1 hour after radiation (IR; middle panels) in GFP- or YAP-transduced CGNPs. YAP-expressing CGNPs showed a higher mitotic ratio (%P-Hist3 positive of treated / % P-Hist3 positive untreated) (bottom right), indicating failure of the G2/M checkpoint in these cells. Again, irradiated GFP-transduced cells were normalized to non-irradiated GFP-transduced CGNPs; irradiated YAP-transduced CGNPs were normalized to non-irradiated YAP-transduced CGNPs. Statistically significant differences are indicated as (*) $P < 0.05$; (***) $P < 0.001$.

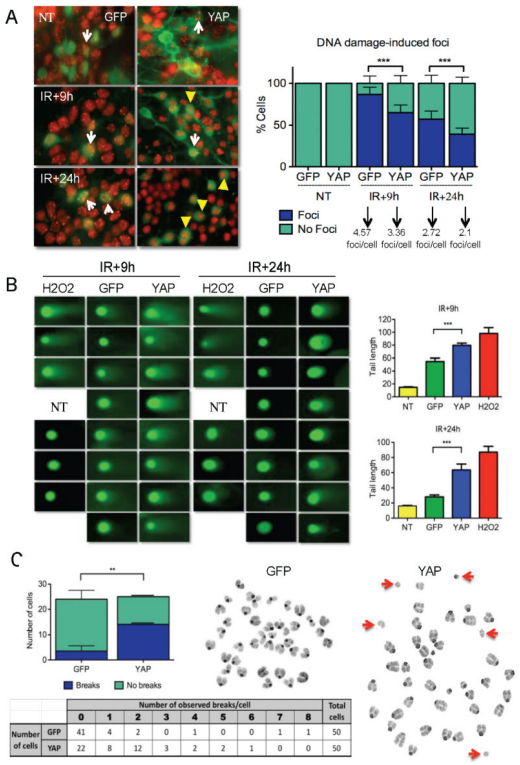

Figure 3. YAP over-expression prevents complete DNA repair

(A) Immunostaining (left) for 53BP1, which marks sites of DNA damage ("foci") in control (NT) or irradiated (IR) CGNPs infected with either GFP or YAP. Quantification shown at right indicates that fewer YAP-transduced cells contained foci compared to GFP-transduced CGNPs, and YAP-transduced cells contained fewer foci/cell.

(B) Comet assay to detect DNA damage performed in CGNPs 9 and 24 hours post-irradiation. H_2O_2 serves as a positive control for detection of damaged DNA by this assay. YAP-over-expressing cells contained more damaged DNA at both time points, as measured by the length of the comets' tails (quantification at right).

(C) (Left) Quantification of chromatid and chromosome breaks in metaphase spreads from GFP- or YAP-transduced CGNPs twenty-four hours after irradiation. Right, representative image of metaphase spreads from GFP- or YAP-transduced irradiated CGNPs; arrows show examples of broken chromosomes. Table summarizes the number of breaks/cell after analysis of 50 irradiated GFP- or YAP-transduced CGNPs. YAP-transduction was also associated with increased genomic instability in a mouse medulloblastoma cell line (Supplementary Figure 3B).

Statistically significant differences are indicated as (**) $P < 0.01$; (***) $P < 0.001$.

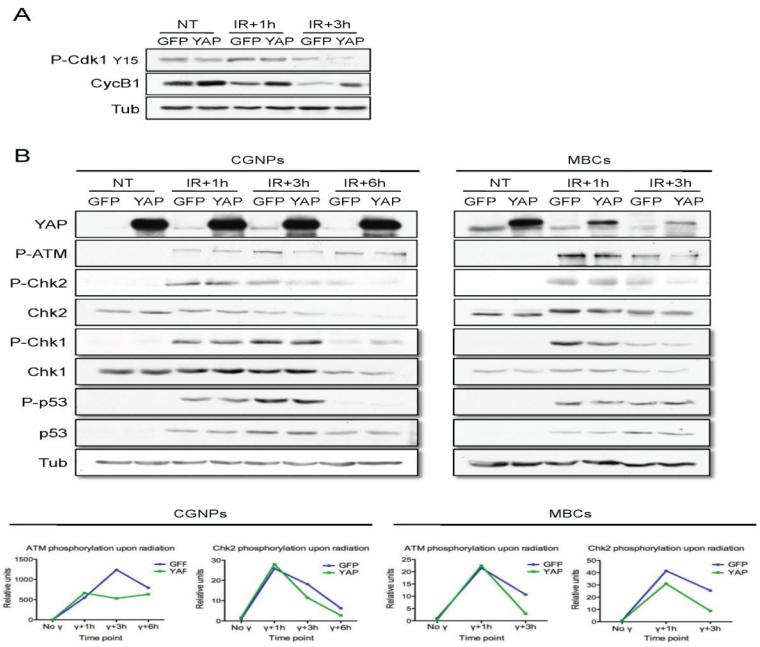

Figure 4. The ATM-Chk2 DNA damage response pathway is rapidly deactivated in YAP over-expressing cells

(A) Representative western blot analysis of GFP- or YAP-transduced CGNPs at the indicated time points after irradiation. CGNPs over-expressing YAP at one and three hours post-irradiation showed reduced levels of inhibited (Tyr-15 phosphorylated) Cdk1, and higher levels of cyclin B1 indicating increased entry into mitosis.

(B) Western blot analysis of GFP- or YAP-transduced CGNPs (left) or NeuroD2-SmoA1 cells (MBCs) (right) at the indicated times after irradiation. YAP-transduced CGNPs show lower levels of phosphorylated ATM and Chk2 3 hours after radiation, compared to GFP-transduced cells. Similar results were observed in irradiated MBCs transduced with either GFP or YAP. Quantification of phosphorylated ATM and Chk2 levels are shown at the bottom. YAP expression did not differentially affect chk1 or p53 levels or phosphorylation.

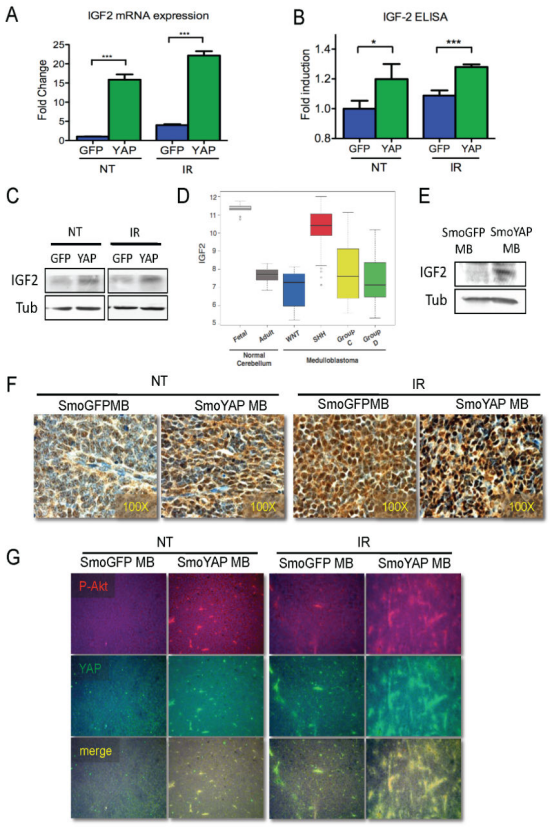

Figure 5. YAP induces expression of IGF2 and activation of Akt

(A) IGF2 was found to be up-regulated in the presence of YAP using microarray analysis, confirmed by quantitative RT-PCR. Irradiation induces IGF2 in GFP- and YAP-infected cells, but levels are significantly higher in YAP-infected CGNPs 3 hours post-irradiation.

(B) ELISA analysis of IGF2 production in GFP- or YAP-transduced control or irradiated CGNPs (3h). Statistically significant differences are indicated as (*) $P < 0.05$; (***) $P < 0.001$.

(C) Western blot analysis of IGF2 protein in GFP- or YAP-transduced control and irradiated CGNPs (3h).

(D) Box plot showing IGF2 mRNA expression obtained from exon array profiling of 103 primary human medulloblastomas, 9 fetal and 5 adult human control cerebella. IGF2 is highly expressed specifically in SHH-driven medulloblastomas (T test, p=3.553E-14). IGF1 is not specifically elevated in human SHH-associated medulloblastomas (Supplementary Figure 4).

(E) Western blot analysis of IGF2 protein in GFP-SmoA1 and YAP-SmoA1 mouse medulloblastomas.

(F) Immunohistochemical staining for IGF2 in medulloblastomas from non-irradiated (left) and irradiated (3h; right) GFP-SmoA1 and YAP-SmoA1 tumor bearing mice.

(G) Immunofluorescence analysis of Akt S473 phosphorylation and YAP protein in medulloblastomas from non-irradiated (left) and irradiated (3h; right) GFP-SmoA1 and YAP-SmoA1 tumor bearing mice.

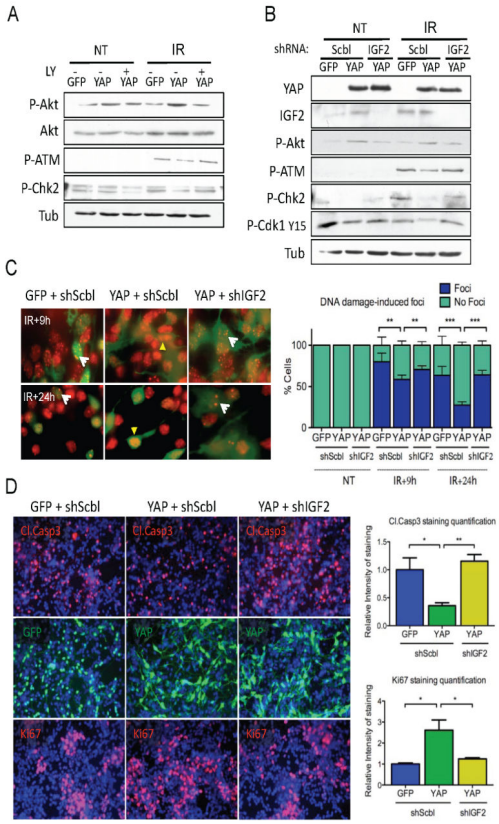

Figure 6. Akt inhibition or IGF2 knock-down abrogate the effects of YAP on DNA repair, proliferation, and survival

(A) Western blot analysis of CGNPs infected with either GFP or YAP, treated with the PI3K inhibitor *LY* 294002 or with vehicle, irradiated and analyzed three hours after radiation. LY 294002 treatment in YAP-expressing cells restored the levels of phosphorylated-Akt, -ATM, and -Chk2 to the levels observed in GFP-expressing CGNPs.

(B) Western blot showing effective knock-down of IGF2 in CGNPs infected with either GFP or YAP, then transduced with lentiviruses targeting IGF2 for short hairpin RNA-mediated knock-down or encoding for a scrambled shRNA sequence. IGF2 knockdown reduces Akt phosphorylation and rescues ATM and Chk2 phosphorylation in YAP-transduced cells 3 hours after irradiation.

(C) Immunofluorescence analysis of 53BP1 localization to foci in irradiated GFP- or YAP-transduced CGNPs subsequently infected with retroviruses targeting IGF2 for short hairpin RNA-mediated knock-down or encoding for a scrambled shRNA sequence. Quantification is shown at right. Fewer YAP-transduced CGNPs contained foci 9 and 24 hours post-irradiation compared to GFP-transduced CGNPs. IGF2 knock-down restored the percentage of cells containing DNA damage-induced foci to the levels observed in GFP-expressing CGNPs.

(D) Immunofluorescence analysis of cleaved caspase 3 and Ki67 in GFP- or YAP-transduced CGNPs infected with either scrambled or IGF2-targeting retroviruses, three hours after irradiation. IGF2 knock-down restored the levels of proliferation and apoptosis to those observed in GFP-expressing CGNPs.

Statistically significant differences are indicated as (*) $P < 0.05$; (**) $P < 0.01$; (***) $P < 0.001$.

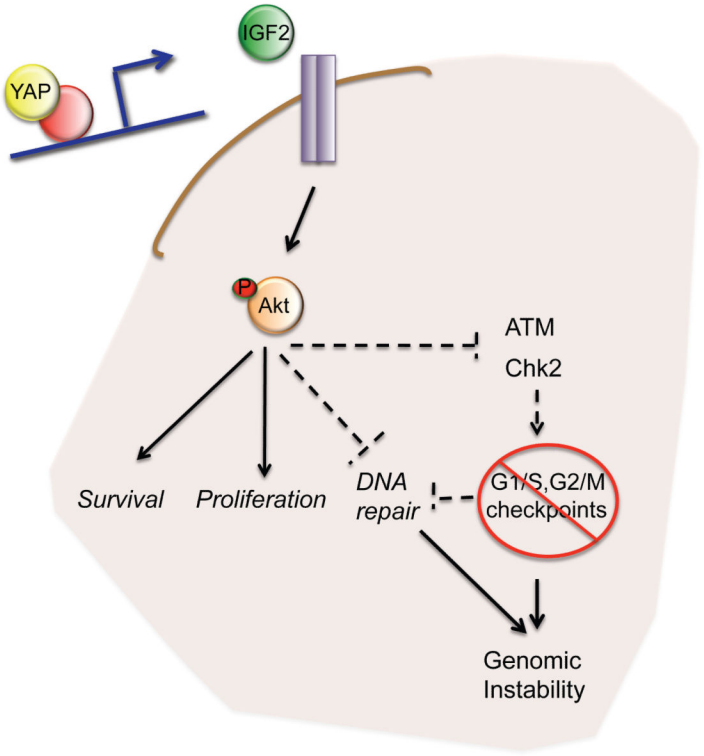

Figure 7. YAP-mediated IGF2 expression drives cell survival, proliferation and genomic instability

Model suggesting the mechanism through which oncogenic YAP expression permits cell proliferation and survival after radiation-induced DNA damage. YAP induces IGF2 expression in CGNPs and medulloblastoma cells. IGF2 activates the PI3K/Akt pathway, promoting survival and increasing proliferation of these cells. In addition, increased activation of Akt leads to faster ATM and Chk2 dephosphorylation after radiation, subsequently deactivating the DNA damage response and removing the G1/S and G2/M checkpoints. Favoring survival, proliferation and genomic instability confers an advantage to YAP-expressing tumor cells. Inhibiting IGF2/Akt signaling in tumors with high YAP expression may prevent recurrence and enable use of lower radiation doses by increasing tumor cell radiosensitivity.